BIOCELL
2021 45(3): 627-638

Tech Science Press

MiR-16-5p plays an inhibitory role in human non-small cell lung cancer through Fermitin family member 2

Junqi GUO[1,2,#]; Yun YANG[1,2,#]; Wei ZHAO[1,2]; Zhonghai YAN[3]; Xia YANG[4]; Yunfei YAN[1,2]; Ruimin HAO[1,2]; Jinxia HU[1,2,*]; Fei JIAO[1,2,*]

[1] Department of Biochemistry and Molecular Biology, Binzhou Medical University, Yantai, 264003, China
[2] Key Laboratory of Tumor Molecular Biology in Binzhou Medical University, Yantai, 264003, China
[3] Department of Neurology, Columbia University, New York, 10032, USA
[4] Department of Cardiology, The People's Hospital of Zhaoyuan City, Yantai, 265400, China

Key words: miR-16-5p, Non–small-cell lung cancer (NSCLC), Fermitin family member 2 (FERMT2), Apoptosis, Invasion, Overall survival (OS)

Abstract: Increasing evidence indicates that aberrant expressions of some microRNAs are associated with cancer progression. However, the roles and biological mechanisms of miRNA-16-5p in human non-small cell lung cancer (NSCLC) are not to be well studied. Here, we validated that the expression of miR-16-5p was decreased significantly in NSCLC samples and cell lines. The correlation between the clinicopathological features of NSCLC and the miR-16-5p expression showed that the expression of miR-16-5p in non-small cell lung cancer was linked with the advanced TNM stage, positive lymph node metastasis, with short overall survival (OS). Also, a negative correlation between miR-16-5p and Fermitin family member 2 (FERMT2) was observed, implying there may be a potential link about their regulation. The hypothesis was further confirmed by in-silico analysis and dual-luciferase reporter assay. Moreover, we demonstrated that the transfections of miR-16-5p mimics could alter some biological characteristics of NSCLC cells remarkably accomplished by the expression variance of FERMT2 *in vitro* and *in vivo* assays. Summarily, this study demonstrated that miR-16-5p, as a tumor suppression factor in NSCLC by targeting FERMT2, could serve as one promising biomarker in the prediction for NSCLC patients.

Abbreviations

NSCLC:	non–small-cell lung cancer
miRNAs:	microRNAs
OS:	overall survival
miR-16-5p:	miRNA-16-5p
FERMT2:	Fermitin family member 2
GAPDH:	glyceraldehyde 3-phosphate dehydrogenase
3'-UTR:	3'-untranslated region
MTT:	3-(4,5-dimethylthiazol-2-yl)-2,5-diphenyltetrazolium bromide
EMT:	epithelial-mesenchymal transition
q-PCR:	quantitative-polymerase chain reaction
FACS:	fluorescence activated cell sorting.

Introduction

Lung cancer is one of the most severe malignant tumors and one of the leading causes of cancer-related deaths in the world. Non–small-cell lung cancer (NSCLC) accounts for about 80% of clinical cases of lung cancer. To date, surgery is the most effective treatment for NSCLC. However, most patients are diagnosed at the later or metastatic stages and lost the chance for operation. The 5-year survival rate after diagnosis is only maintained at 16.6% (Lewis *et al.*, 2018). Because of the difficulties in early diagnosis of the disease, NSCLC is still a significant challenge for public health.

MiRNA is a small non-coding RNA molecule with a length of about 17–25 nucleotides to boost the degeneration of mRNAs or suppress the mRNA translation by binding to the 3'-untranslated regions (3'-UTRs) of mRNAs, thus promoting the degradation of mRNA (Bentwich *et al.*, 2005). To date, about 2500 miRNAs have been identified in humans (Kozomara and Griffiths-Jones, 2011). It has been well-known that quite a few miRNAs serve as practical and safe markers for cancer detection (Li *et al.*, 2018; Yan *et al.*, 2017). Similarly, some

*Address correspondence to: Jinxia Hu, hujinxia@bjmu.edu.cn; Fei Jiao, slytjiaofei@bzmc.edu.cn
#These authors contributed equally to this work.
Received: 08 August 2020; Accepted: 25 September 2020

Doi: 10.32604/biocell.2021.013496

miRNA signatures have been successfully applied to the screening or diagnosis of lung cancer (Croce, 2009). As a tumor-suppressive factor, miRNA-16-5p (miR-16-5p) is recognized to be deregulated in many malignant cells such as breast cancer (Li *et al.*, 2018; Qu *et al.*, 2017), retinal leukostasis (Ye *et al.*, 2016), chordoma (Zhang *et al.*, 2018), pituitary adenoma (Renjie and Haiqian, 2015), gastric carcinoma (Wang *et al.*, 2017b), prostate cancer (Hao *et al.*, 2016), ovarian cancer (Pero-Gascon *et al.*, 2018; Yan *et al.*, 2017), colon cancer (Shi *et al.*, 2014) as well aschronic lymphocytic leukemia (CCL) (Pekarsky and Croce, 2015). However, the role of miRNA-16-5p in NSCLC has not been fully elucidated.

Cell adhesion to the cellular matrix is crucial for cell immobilization, especially in solid tissues. At the beginning of the tumor, cells begin to aggregate and adhere to the substratum. With the development of the tumor, cells invade into the cellular matrix, thus allowing cancer to acquire metastasis characteristics (Kloeker *et al.*, 2004). FERMT2, also named as Kindlin2, is a focal adhesion protein involved in tumor development and progression through the interaction with integrins, especially integrin beta1 (Rognoni *et al.*, 2016). Although there are many studies reported that FERMT2 prompted epithelial-mesenchymal transition (EMT), which connected closely with cancer cell migration, invasion, and metastasis (Lu *et al.*, 2018), the mechanisms of its regulation need to be further ascertained.

In this study, we identified the expression of miR-16-5p and FERMT2 in clinical samples and cultured cell lines and then performed the correlation between the miR-16-5p and some clinicopathological parameters in NSCLC patients. As a negative correlation between miR-16-5p and FERMT2 was established, we further tested the hypothesis that FERMT2 could be guided by miR-16-5p in NSCLC cells. Bioinformatics analysis was further performed to verify FERMT2 as one probable target of miR-16-5p. The luciferase reporter assays further corroborated that FERMT2 is a direct target of miR-16-5p. Also, our results exhibit that the overexpression of miR-16-5p could influence some biological characteristics of NSCLC cell lines. Furthermore, the cotransfection of FERMT2 without 3'-UTR rescued the effects of miR-16-5p expression in NSCLC cells. The present study provided evidence that miR-16-5p exhibited an anti-cancer effect by targeting FERMT2 in NSCLC.

Materials and Methods

Statement of ethics

All experiments and assays for human samples and cell tissue were performed at Binzhou Medical University. Access to the relevant de-identified patient tissues and analysis of patient data was approved by the Institutional Review Board for Human Research at Binzhou Medical University. Written informed consent was obtained from all individual participants and the project was approved by the Ethics Board of Binzhou Medical University (approval number: 2019-23); Animal procedures are carried out in strict accordance with guidelines and procedures of the Institutional Animal Care and Use Committee (IACUC) of Binzhou Medical University (No. 2019-23).

Clinical samples

In total, fifty-nine eligible NSCLC patients (33 males and 26 females) were enrolled at Yantai Shan Hospital, Binzhou Medical University, from June 2011 to July 2012. The lung cancer tissues and matched healthy tissues were derived from adult patients who had pathologically diagnosed as NSCLC and no adjuvant therapies before surgery, including chemotherapy, immune therapy, and radiotherapy. All patients were followed up after the operation, and their clinicopathological features were summarized and analyzed in Tab. 1. The overall survival (OS) was plotted according to the algorithm of Kaplan-Meier, and the *log-rank test* was applied to compare the OSs between groups. All the specimens were maintained at −80°C for further analyses.

Cell culture

For *in vitro* tests, three human lung cell lines were used, including one standard bronchial epithelial cell line (HBE cells) and two NSCLC cell lines (A549/H1299 cells). All three cell lines were purchased from the Cell Bank of Type Culture Collection of Shanghai Institute of Cell Biology, Chinese Academy of Sciences. And the cell lines were cultured in RPMI-1640 medium (Gibco, USA) supplemented with 10% (v/v) fetal bovine serum (FBS) (Gibco, USA) at 37°C in a humidified 5% CO_2 incubator. 293T cells were also obtained from ATCC (Chinese Academy of Sciences, Shanghai) cultured with DMEM medium containing 10% FBS at 37°C under 5% CO_2.

Transfection

During transfections, both A549/H1299 cells were treated with miR-16-5p scram (Scram group, 50 nM), miR-16-5p mimics (Mimics group, 50 nM), and miR-16-5p mimics + FERMT2-without-3'-UTR (Rescue group, 50 nM), respectively. Briefly, cells were seeded into 6-well plates at a density of 200,000 cells/well and allowed to attach overnight until reaching about 70–80% confluence. The scram and mimics of miR-16-5p were synthesized by Shanghai GenePharmaCo., Ltd. (Shanghai, China). Cell transfections were performed with Lipofectamine™ 2000 (Life Technologies; Thermo Fisher Scientific, Inc.) using the manufacturer's protocol. After incubation for 8 h, the medium was replaced with the standard culture medium containing 10% FBS. After 48 h, cells with different treatments were harvested for further analyses.

Cell proliferation assays

For colony formation assays, 1.5×10^3 cells with different treatments were seeded into each 10-cm plate. The plates were fixed with 100% methanol and stained in 20% ethanol containing 0.2% crystal violet dye two weeks later. Then, the numbers of colonies were analyzed. For MTT assays, the detection was performed according to the instrument of the manufacturer (Beyotime Biotechnology, cat. no. C0009). Briefly, 6×10^3 cells were seeded into 96-well plates in triplicate and treated with 10 μL reagents for further incubation 4 h. After 150 μL detergent reagents were added into wells, the absorbance was detected in the microplate reader at 570 nm wavelength.

Apoptosis and flow cytometry cycle analysis

For apoptosis analysis, cells with different treatments were harvested after 48 h, and the oligonucleotides were transfected into NSCLC cells, then washed twice with cold PBS, suspended the cells with the buffer then double-stained with Annexin

TABLE 1

Chi-Square analysis of the association of clinicopathological features and the miR-16-5p expression in NSCLC patients (N = 59)

Clinicopathological features	Patients (n = 59)	miR-16-5p in NSCLC patients		*p*-Value
		Low (n = 36) n (%)	High (n = 23) n (%)	
Age (years) ≦60	22	13 (36.1)	9 (39.1)	0.815
>60	37	23 (63.9)	14 (60.9)	
Gender				0.642
Male	33	21 (58.3)	12 (52.2)	
Female	26	15 (41.7)	11 (47.8)	
Smoker				0.909
Non	20	12 (33.3)	8 (34.8)	
Previous or current	39	24 (66.7)	15 (65.2)	
Tumor size				0.964
≦3 cm	31	19 (52.8)	12 (52.2)	
>3 cm	28	17 (47.2)	11 (47.8)	
TNM stage				0.003
Early (I/II)	20	7 (19.4)	13 (56.5)	
Advanced (III/IV)	39	29 (80.6)	10 (43.5)	
Pathology				0.498
Adenocarcinoma	25	14 (38.9)	11 (47.8)	
Squamous cell carcinoma	34	22 (61.1)	12 (52.2)	
Node metastasis				<0.001
Negative	26	9 (25.0)	17 (73.9)	
Positive	33	27 (75.0)	6 (26.1)	

Note: Abbreviations: NSCLC, non-small cell lung cancer; TNM, tumor (T), the extent of spread to the lymph nodes (N), and the presence of metastasis (M).

V-FITC (5 μg/mL) and PI (5 μg/mL) (BD Pharmingen; NJ, USA). For cell cycle analysis, cells with different treatments were washed with cold PBS and then fixed in cold 75% ethanol (v/v) followed by 1h incubation on ice and 24 h incubation at −20°C. Fixed cells were resuspended in PBS containing RNase A (50 μg/mL) for 30 min, then added PI (50 μg/mL). Finally, both the apoptosis and cell cycle were analyzed by FACS (Beckman Coulter Flow Cytometer, CA, USA).

Cell invasion assays

Transwell assay was used to detect the migration and invasion abilities of A549/H1299. Briefly, 1×10^6 cells in 100 μL serum-free medium were added into the upper chamber of 24-well plates directly. Serum-containing media (20% FBS, 600 μL) served as a chemical attractant in the lower chambers. The upper chamber was taken after 48 h, and non-migrated cells were swapped by a cotton plug. Cells at the bottom of the membrane were then fixed with methanol stained with crystal violet and observed the sample under a microscope (Olympus, Tokyo, Japan). The number of invasive or migrated cells was discerned by calculating ten randomly selected fields of stained cells with ImageJ software.

Quantitative-polymerase chain reaction (q-PCR)

For miR-16-5p expression analysis, small RNAs were isolated from cells from different groups with RNAiso Plus (Takara Biotechnology. Dalian, China) in which human 5S rRNA acted as the positive endogenous references. For the expression analyses of related genes, total RNA was isolated using TRIzol reagent. qPCR was performed with SYBR-Green PCR Master Mix (Applied Biosystems, Foster City, CA, USA) on an RG3000 System (Qiagen GmbH, Hilden, German), GAPDH was used as an endogenous control. The relative gene expression levels were calculated as relative quantification ($2^{-\Delta\Delta Ct}$) method. All experiments were performed in triplicate. The primers used in this study are listed below:

miR-16-5p: F5'-ACACTCCAGCTGGGTAGCAGCACG TAAATA-3'
R5'-AACATGTACAGTCCATGGATG-3'
5S rRNA: F5'-GTTGTCTCCTGCGACTTCA-3'
R5'-GGTGGTCCAGGGTTTCTTA-3'
FERMT2: F5'-TATCATTTTATCATGAAAACTTCTT-3'
R5'-GACTTTATCACCCGTTTA-3'
GAPDH: F5'- GTTGTCTCCTGCGACTTCA-3'
R5'- GGTGGTCCAGGGTTTCTTA-3'

Western blot analysis

Total protein was extracted from the lung carcinoma cells by RIPA lysis buffer (Solarbio, Beijing, China) and then quantified. Subsequently, the protein was separated by 10% SDS-PAGE, followed by transferring to the PVDF membrane (Sigma-Aldrich, USA) and then blocked in 5%

non-fat skimmed milk at room temperature for 1 h. The PVDF membrane was incubated with the primary antibodies (1:1000) overnight at 4°C. The rabbit antibodies (LI-COR, C60405-05, USA) were added to the PVDF membrane after primary incubation. Finally, Tanon 5200 was used to detect the protein expression signal. The primary antibodies for detection were as follows: rabbit antibodies against FERMT2 (Abcam, cat. no.ab127745), GAPDH (Bioworld Technology, cat. no. AP0063), cleaved caspase-3 (Cell Signaling, cat. no. 9661), cleaved caspase-8 (Cell Signaling, cat. no. 9748) and cleaved caspase-9 (Cell Signaling, cat. no. 9505), Bcl-2 (Bioworld Technology, cat. no. BS1511), Bax (Bioworld Technology, cat. no. BS2538), p-Rb (Bioworld Technology, cat. no. BS4164), MMP-2 (Thermo Scientific, cat. no. MA5-14186), MMP-9 (Thermo Scientific, cat. no. MA5-13595), GAPDH as a loading control for protein normalization. The intensity of each protein in Western blot was normalized to internal control of GAPDH with ImageJ software and expressed as a ratio of the densitometric value.

Plasmid construction and luciferase reporter assay

Prediction of miRNA target genes was performed using the TargetScan 5.2 (http://www.targetscan.org/) databases. The sequence of FERMT2 (NM_006832.3) was obtained from GenBank. The primers to amplify the 3'-UTR of FERMT2 (wild type or mutant) were commercially synthesized (Shanghai GenePharma Co., Ltd.). The DNA from 293T cells served as the amplification template. Then, either wild-type FERMT2 or its mutant fragment was inserted in the vectors of pMIR-REPORT miRNA Expression Reporter Vector System (RN: R10032.4 Guangzhou RibBio Co., LTD) and were termed FERMT2-3'-UTR-WT and FERMT2-3'-UTR-MUT, respectively. The 293T cells were plated in 96-well plates at a density of 7×10^3 cells triplicate in 100 μL/well, then transfected with miR-16-5p scram/mimics (50 nM, Suzhou GenePharma) together with wild-type/mutated luciferase reporter vector by Lipofectamine 2000 (Invitrogen, Thermo Fisher Scientific. CA, USA). Cells were harvested after 48 h, and the luciferase activities were detected by Luci-Pair Duo-Luciferase Assay kit 2.0 (GeneCopoeia, Rockville, USA).

Tumor growth in nude mice

The A549 cells (1×10^6) with different treatments were resuspended in 150 μL PBS and then injected subcutaneously into the back of nude mice (the left for the scram group and the right for the mimics group, respectively). The tumor growth curve was made to observe the effects of miR-16-5p on tumor formation and growth *in vivo*. The size of the tumor was recorded every three days. The formula V (mm^3) = ($L \times W^2$)/2 was used to calculate the amount, where L is the long axes of the tumor, and W indicates the short axes individually. On the 30th day, mice were sacrificed via cervical vertebra dislocation, and the tumor masses were harvested and weighed. The removed tumors were snap-frozen for future use.

Statistical analysis

All detections were performed at least in triplicate, and all data are represented as the mean ± standard error (SE). The statistical comparisons were analyzed using Student's *t*-test for two groups and ANOVA for three or four groups. The association of NSCLC patients' clinicopathological parameters and their miR-16-5p expression in NSCLC tumors was performed by Chi-squared analysis. Kaplan–Meier model with a *log-rank test* was implemented to compare the NSCLC patients' overall survival distributions. All statistical analyses were performed with SPSS 22.0 (IBM Corp, NY, USA). A test with *p*-values less than 0.05 was considered statistically significant.

Results

Reduction of the expressions of miR-16-5p in NSCLC

Firstly, the small RNAs from NSCLC samples and their healthy counterparts were isolated to determine the differences in miRNA expression between cancer and normal healthy tissues. The results of qPCR indicated the expressions of miR-16-5p is decreased in NSCLC tissues compared with that in healthy counterparts (Fig. 1A). The NSCLC patients were classified into two subgroups based on the median expression level of miR-16-5p in tumors, which included 36 patients with low expression levels and 23 patients with high expression levels, respectively. Subsequently, we followed up 59 patients and recorded a total survival (OS) of up to 60 months after their operation. The OS was plotted based on the Kaplan-Meier algorithm, and the *log-rank* test was addressed to analyze OSs between patients with low NSCLC miR-16-5p and those with high NSCLC miR-16-5p. The analysis of the *log-rank* test demonstrated that the OS of patients with low miR-16-5p was remarkably worse than that of patients with higher miR-16-5p (Fig. 1B, $p = 0.0026$, *log-rank test*). Moreover, the results of Western blot showed FERMT2 was much higher in cancer tissues than that in the regular counterparts (Figs. 1C and 1D), with significant statistical differences between the two groups. These data suggested that there may be a negative correlation between miR-16-5p and FERMT2 expressions during the tumorigenesis of NSCLC, which has been verified by the correlation analysis (Fig. 1E).

The association between miR-16-5p expression with the clinicopathological features in NSCLC patients

To evaluate whether miR-16-5p can be used as an index of prognosis in patients with NSCLC, the association of miR-16-5p expression and the critical clinicopathological indexes of patients was discussed. All 59 patients were classified based on the median expression level of miR-16-5p into the elevated group (N = 23) and low group (N = 36). The Chi-squared analysis showed that some of the clinicopathological parameters were not correlated with miR-16-5p expression in NSCLC patients, such as age, gender, smoking history, tumor size, and cancer histology (Tab. 1, $p < 0.05$). In contrast, we found that the TNM stage and lymph node metastasis in NSCLC patients with low miR-16-5p were significantly different from those in patients with high endogenous miR-16-5p (Tab. 1, $p < 0.01$).

miR-16-5p suppresses FERMT2 expression in NSCLC through binding to its 3'-UTR

Bioinformatics analysis was first carried out by TargetScan to find out the potential target of miR-16-5p. The prediction results show that there are some complementary sequences between 3'-UTR of miR-16-5p and FERMT2, indicating that

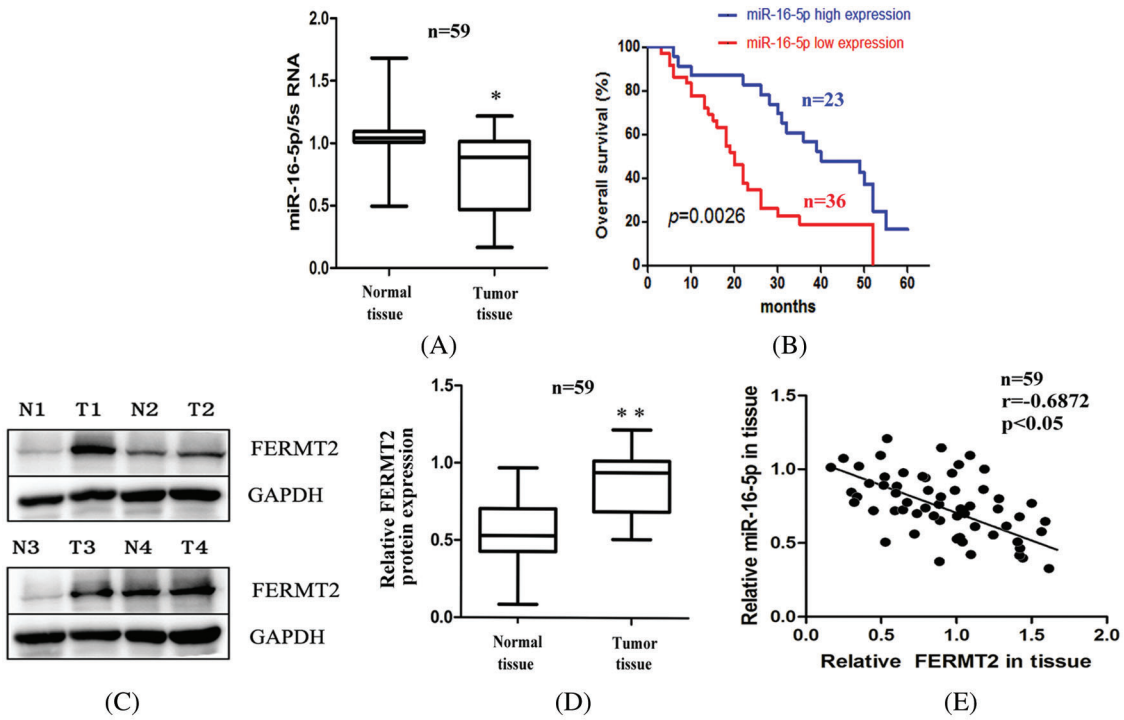

FIGURE 1. The detections of miR-16-5p and FERM2 expression in tissues.
(A) A comparison of the relative expression level of miR-16-5p in normal and tumor tissues determined by qRT-PCR. (B) Correlation of miR-16-5p expression with overall survival (OS) of NSCLC patients. Among 59 patients with NSCLC, the overall survival was plotted to compare OS between patients with low miR-16-5p and those with high miR-16-5p ($p = 0.0026$, *log-rank test*). (C) Representative results of FERMT2, tested by Western blot in normal and tumor tissues. (D) The quantified analyses of FERMT2 levels in normal and tumor tissues, detected by Western blot. (E) The correlation analysis between the expressions of miR-16-5p and FERMT2 protein in clinical NSCLC samples. N: Normal tissue, T: tumor tissue. $^{*}p < 0.05$, $^{**}p < 0.01$.

FERMT2 may be a prospective target of miR-16-5p (Fig. 2A). To test that FERMT2 could be a direct target of miR-16-5p, we cloned dual-luciferase reporter vectors, FERMT2-3'-UTR-WT and FERMT2-3'-UTR-MUT, and cotransfected with the mimics of miR-16-5p into 293T cells for 48 h. The results of dual-luciferase reporter assays showed that miR-16-5p mimic significantly inhibited the luciferase activity of FERMT2-3'-UTR-WT. Conversely, there were no substantial changes in the luciferase activity from cells transfected with FERMT2-3'-UTR-MUT (Fig. 2B), indicating miR-16-5p can regulate the FERMT2 expression through binding to its 3'-UTR.

To elucidate the possible roles of miR-16-5p in NSCLC, the potential mechanistic link between miR-16-5p and FERMT2 was further determined. To this end, we additionally detected the miR-16-5p expression in three cell lines (HBE, A549, and H1299), respectively. The results showed that miR-16-5p was obviously reduced in A549/H1299 cells compared with that in HBE cells (Fig. 2C). Subsequently, the mimics of miR-16-5p were synthesized and transfected into A549/H1299 cells for further investigation. The quantitative real-time PCR indicated they could influence the miR-16-5p expression evidently in both cells (Fig. 2D). It has also been investigated that whether the transfections of miR-16-5p mimics could alter the expression of FERMT2. The results demonstrated that the miR-16-5p could significantly down-regulate the expression of FERMT2 at both mRNA and protein levels (Figs. 2E–2G). These results further revealed that FERMT2 is a candidate target of miR-16-5p.

miR-16-5p acts as an inhibitor on colony formation and cell proliferation via FERMT2

We next investigate the role of miR-16-5p in cell proliferation and colony formation. The results from colony formation assay uncover that the upregulation of miR-16-5p notably inhibited the capacity of colony formation in miR-16-5p-mimic-treated A549/H1299 cells compared with the scram cells. Furthermore, the cotransfection of FERMT2 without 3'-UTR can significantly rescue the suppressive competence of miR-16-5p on colony formation of both cells (Figs. 3A and 3B). For MTT assay, we observed an apparent decrease in cell viability in both A549/H1299 cells following miR-16-5p-mimics treatment. Similarly, the effects of miR-16-5p on the proliferation of two cells can be significantly reversed by the cotransfection of FERMT2-without-3'-UTR (Fig. 3C). Overall, these results revealed that miR-16-5p might act as a suppressive regulator via FERMT2 for the propagation of A549 and H1299 cells.

miR-16-5p influences the apoptosis, cell cycle, and invasion via FERMT2

The effects of miR-16-5p on cell apoptosis and cell cycle distribution were observed by flow cytometry. As shown in Figs. 4A and 4B, miR-16-5p mimics could significantly increase the apoptosis of A549/H1299 cells. On the contrary, the treatment of FERMT2-without-3'-UTR could dramatically reverse the effect of miR-16-5p on the apoptosis of both cells. It suggested that miR-16-5p may promote the apoptosis of NSCLC cells through FERMT2.

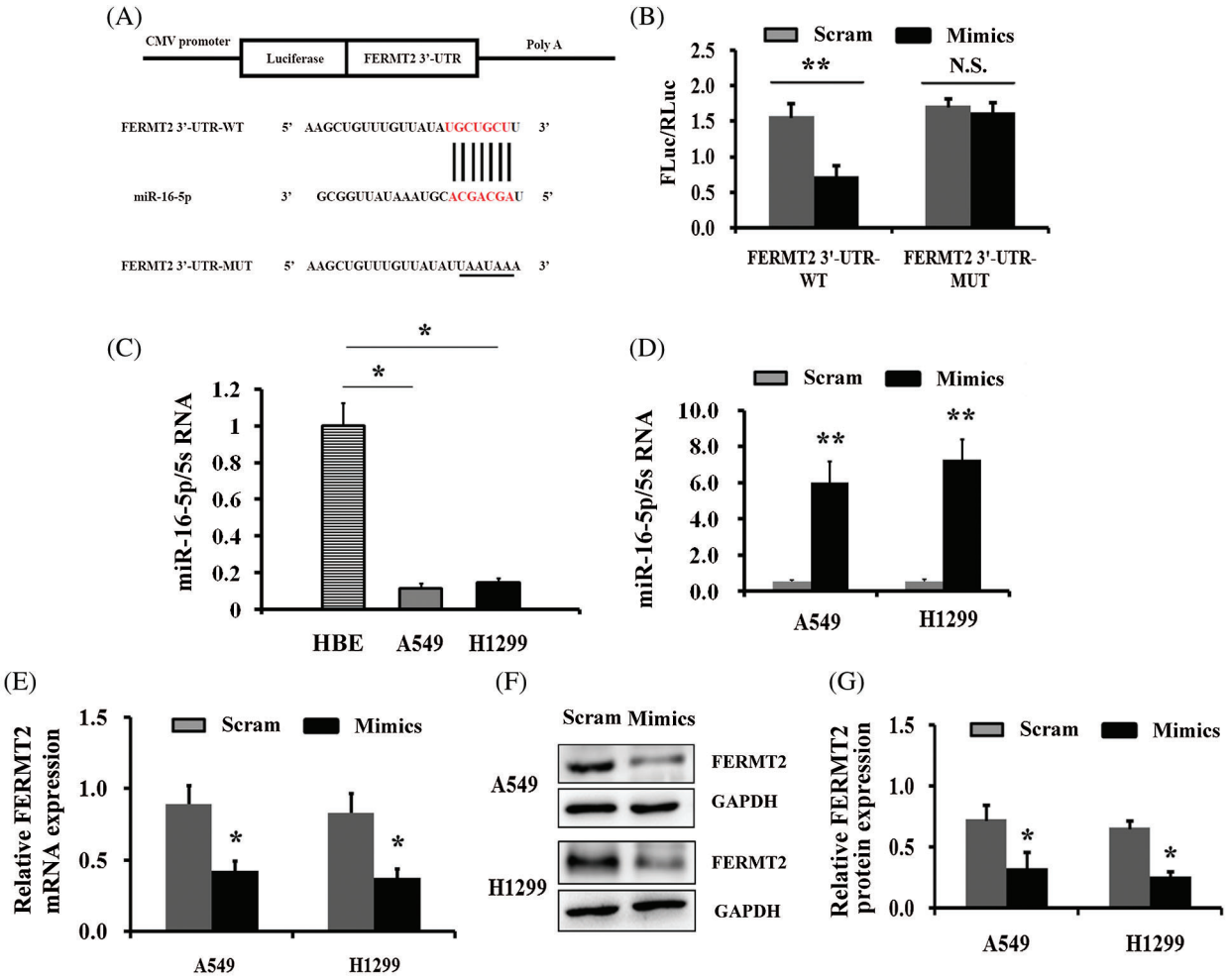

FIGURE 2. miR-16-5p targeted FERMT2.
(A) The binding sequences of miR-16-5p and FERMT2 were predicted with TagetScan 5.2. (B) Luciferase reporter assay was performed in 293T cells co-transfected with miR-16-5p mimics and FERMT2-3'-UTR-WT/FERMT2-3'-UTR-MUT. (C) The levels of miR-16-5p expression in HBE, A549 and H1299 cells, tested by qRT-PCR analysis. (D) The expressions of miR-16-5p in A549 and H1299 cells transfected with miR-16-5p mimics. (E) The mRNA levels of FERMT2 expression in A549 and H1299 cells transfected with miR-16-5p mimics. (F) The protein levels of FERMT2 expression in A549 and H1299 cells transfected with miR-16-5p mimics. (G) The quantified analyses of the FERMT2 protein level in A549 and H1299 cells transfected with miR-16-5p mimics detected by Western blot. *$p < 0.05$, **$p < 0.01$, N.S.: no significance.

The data of cell cycle analysis showed that the cells proportion of A549 and H1299 cells in G_0/G_1 was higher significantly than that from the scram group under miR-16-5p simulation. Conversely, in both cells cotransfected with FERMT2-without-3'-UTR, cells at the G_0/G_1 phase decreased substantially in both A549 and H1299 cells compared with those in the scram group (Figs. 4C and 4D). These results demonstrated that miR-16-5p exhibits a repressive effect on the cell cycle via FERMT2.

To study the effects of miR-16-5p on the invasion of A549/H1299 cells, transwell assays were carried out. Figs. 4E and 4F showed that the number of invaded cells decreased significantly in miR-16-5p mimics treated A549 and H1299 cells compared with the matched scram group. In contrast, the amount of the migrated cells in both A549/H1299 cells co-transfected with FERMT2-without-3'-UTR has no significant difference compared with the scram group (Figs. 4E and 4F).

miR-16-5p affects cell apoptosis-, cell cycle- and invasion-related proteins via FERMT2

To further delineate the mechanisms underlying the miR-16-5p-regulated apoptosis, cell cycle, and invasion in these cells, the expressions of critical genes were assessed by Western blot. As shown in Figs. 5A and 5B, the results showed that the amount of cleaved-caspase3, 8, 9, and Bax increased obviously after the transfection with miR-16-5p mimics at 48 h, while Bcl-2 was downregulated significantly in A549 cells. Because of the key role of P-Rb protein in the transition of G_1 to S phage, the level of P-Rb was detected. A significant decrease of P-Rb in A549cells was observed after the treatment of miR-16-5p mimics. For invasion-related protein, the expression of MMP-2 and MMP-9 were investigated in different groups. The data showed that miR-16-5p mimics could significantly decrease the expression of MMP-2 and MMP-9 in A549 cells. In contrast, the expressions of all these proteins have no significant changes after the cotransfection of FERMT2-without-3'-UTR in A549 cells (Figs. 5A and 5B). Similar results were found in H1299 cells (Figs. 5C and 5D).

miR-16-5p inhibits in vivo *lung cancer growth*

As the results from *in vitro* studies showed that miR-16-5p mimics have significantly suppressive effects on cell proliferation, the anti-tumor effects of miR-16-5p *in vivo*

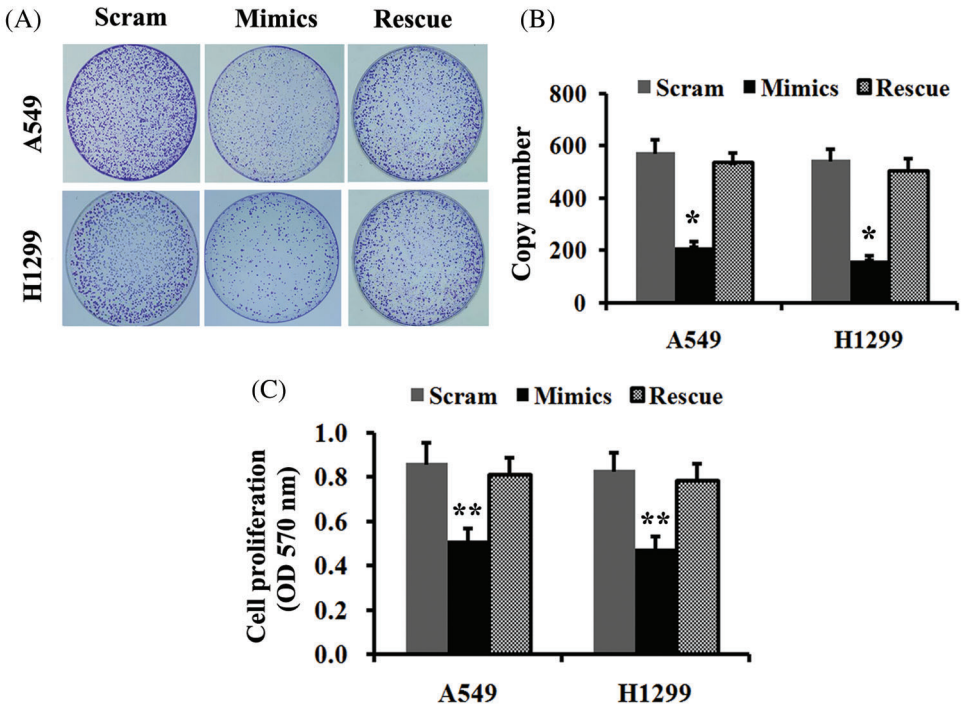

FIGURE 3. The effects of miR-16-5pon the proliferation of A549 and H1299 cells via FERMT2.
(A) Colony formation assays in A549 and H1299 cells transfected with miR-16-5p scram, mimics, and rescue (mimics + FERMT2-without-3'-UTR), respectively. (B) Cell colonies were counted and quantified by the histogram. (C) The MTT assays were performed to assess the viability of A549 and H1299 cells transfected with miR-16-5p scram, mimics, and rescue (mimics + FERMT2-without-3'-UTR), respectively. $^{*}p < 0.05$, $^{**}p < 0.01$.

were further explored. To this end, the tumor growth was evaluated in nude mice with the subcutaneous injection of A549 cells (1×10^6) with or without treatment of miR-16-5p mimics. The tumor volumes of different groups were measured on days 1, 6, 12, 18, 24, and 30, respectively. As shown in Figs. 6A and 6B, the tumor volumes from miR-16-5p-mimics-treated mice were reduced significantly compared with the scram group. At the endpoint (day 30), mice were killed, the tumors were removed in total and weighed. The data confirmed that the tumor weights in the miR-16-5p-mimics-treated group were markedly decreased than those in the scram group (1.59 ± 0.28 g *vs.* 0.67 ± 0.38 g, $p < 0.01$) (Figs. 6C and 6D). Moreover, in the inoculated tumors, the miR-16-5p expression levels increased significantly in the mimics group compared with the scram group (Figs. 6E and 6G). Oppositely, decreased levels of FERMT2 protein were noticed in the mimics group compared with the scram group (Figs. 6F and 6H).

Discussion

Lung cancer has been the leading cause of cancer-related mortality, in which NSCLC accounts for 80–85% of cases (Crino *et al.*, 2010). Though tremendous advances and improvements have been made in the biology and therapeutic strategies of lung cancer, the treatment of lung cancer remains unsatisfactory. To date, considerable evidence has indicated miRNA is closely related to many biological and pathophysiological processes, including cancer (Cai *et al.*, 2018; Cui *et al.*, 2018; Ha, 2011; Paladini *et al.*, 2016). miR-16-5p, as a subgroup of miR-16, is considered to be a candidate miRNA with potential tumor suppressor activity. Several studies have reported that miR-16-5p is involved in the regulation of cell cycle progression, cell proliferation and invasion, and stimulating cell apoptosis (Cimmino *et al.*, 2005; Hanniford *et al.*, 2015; Rinnerthaler *et al.*, 2016; Zhang *et al.*, 2018). Also, a majority of the literature has shown that miR-16-5p can inhibit cell growth in multiple cancer types, including chronic lymphocytic leukemia (Hanniford *et al.*, 2015), prostate cancer (Bonci *et al.*, 2008), hepatocellular carcinoma (Guo *et al.*, 2009), breast cancer (Xu *et al.*, 2010), ovarian cancer (Bhattacharya *et al.*, 2009), gastric cancer (Xia *et al.*, 2008), and multiple myeloma (Corthals *et al.*, 2010). However, the effect of miR-16-5p on NSCLC has not been fully investigated.

In the present study, we set out to detect miR-16-5p expression in NSCLC samples and noticed that it was significantly down-regulated in the tissue of NSCLC compared with healthy counterparts. Also, a significant inverse correlation between miR-16-5p and FERMT2 expressions was revealed in NSCLC samples. The same results were observed in cultured lung cancer cells, such as A549 and H1299 cells. Moreover, miR-16-5p expression in NSCLC patients was associated with some clinicopathological features, such as advanced TNM stages, positive lymph node metastasis, as well as short overall survival. These data demonstrated that miR-16-5p presented the anti-cancer effect of miR-16-5p in NSCLC. To further elucidate whether the miR-16-5p potential functions in NSCLC tumorigenesis and development via FERMT2, a series of assays were carried out to observe the functional changes of miR-16-5p on the biological characteristics with or without of FERMT2-without-3'-UTR cotransfection in A549/H1299 cells. Moreover, in the xenograft model of nude mice, it was found that the induced expression of miR-16-5p can also inhibit tumor proliferation *in vivo*. Our data demonstrated that miR-16-5p could inhibit the proliferation, invasion, migration, as well as induce apoptosis in NSCLC cells via FERMT2.

MiRNA can regulate the target gene expression by recognizing the 3'-UTR, leading to mRNA of target gene decay or translation repression. Undoubtedly, it is the

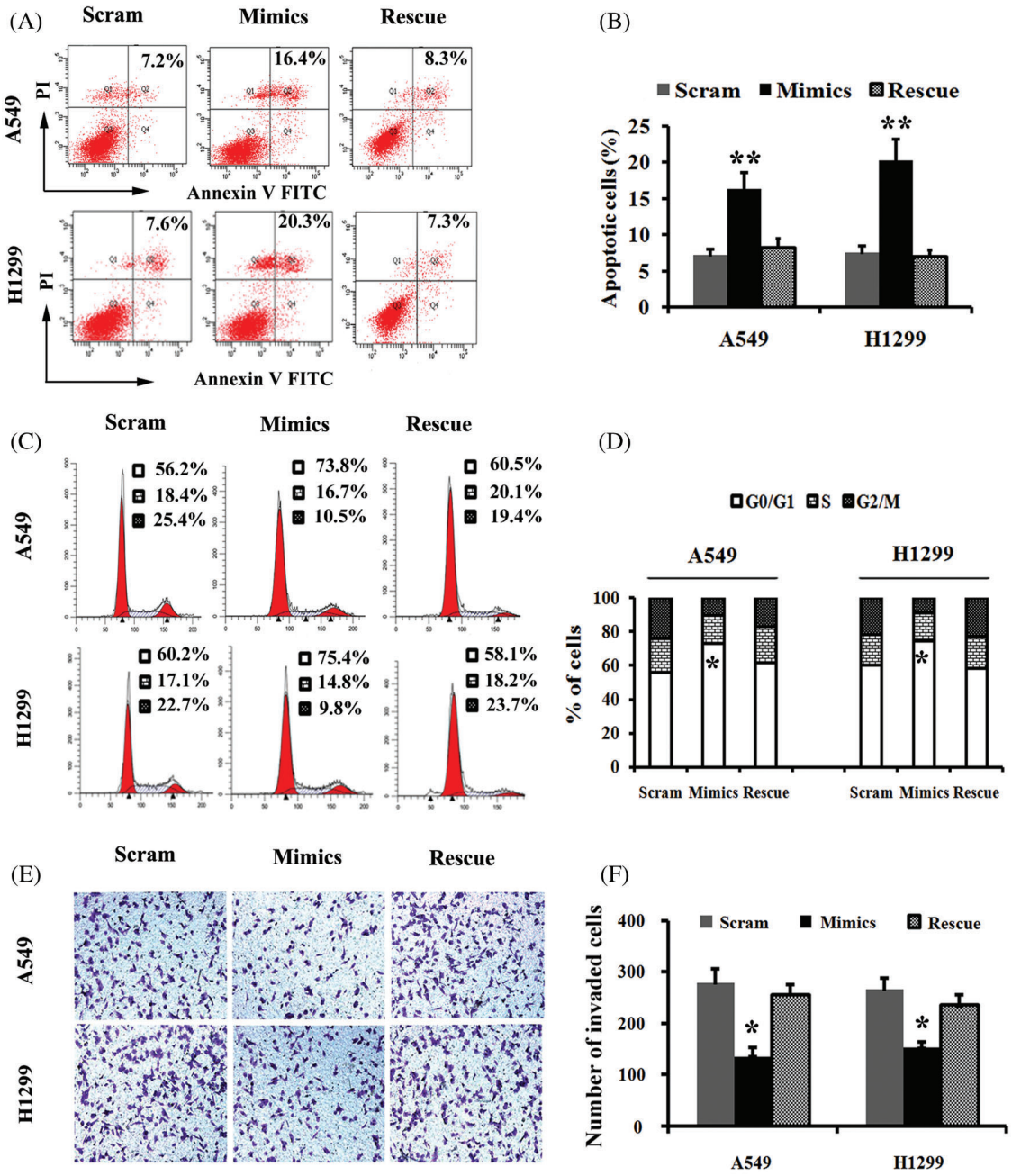

FIGURE 4. The influences of miR-16-5p on the apoptosis, cell cycle, and invasion of A549 and H1299 cells via FERMT2.
(A) The percentages of apoptotic cells were detected in A549 and H1299 cells transfected with miR-16-5p scram, mimics and rescue (mimics + FERMT2-without-3'-UTR), respectively. (B) The percentages of apoptotic cells were quantified by the histogram. (C) The distributions of the cell cycle were detected in A549 and H1299 cells transfected with miR-16-5p scram, mimics and rescue (mimics + FERMT2-without-3'-UTR), respectively. (D) The distributions of the cell cycle were quantified by the histogram. (E) The transwell assays were performed to assess invasion capacity in A549 and H1299 cells transfected with miR-16-5p scram, mimics and rescue (mimics + FERMT2-without-3'-UTR), respectively. (F) The invaded cells were counted and quantified by the histogram. $^{*}p < 0.05$, $^{**}p < 0.01$.

expression changes of target genes of miRNA further trigger the downstream signal cascades related to a broad range of biological processes. Therefore, the identification of specific miRNA target genes is pivotal to elucidate the underlying mechanisms. To date, there have been several studies published recently about the predominant role of miR-16-5p in cancer deterioration. For example, miR-16-5p is reported to suppress the string tumor cells proliferation, invasion, and metastasis by targeting Smad3 (Zhang *et al.*, 2018). Similarly, in breast carcinoma, Qu and his colleagues found the suppressive functions of miR-16-5p in the proliferation and invasion by targeting VEGFA (Qu *et al.*, 2017). In contrast, the regulatory mechanism of miR-16-5p in inhibiting NSCLC cell growth is not elucidated.

FERMTs are evolutionary conserved, focal adhesion proteins that interact with the integrin family, in particular, the integrin beta1 (Kloeker *et al.*, 2004; Rognoni *et al.*, 2016). FERMT2 was the first member of the FERMT family to be discovered. Numerous studies showed that FERMT2 is associated with tumor growth and progression, including breast cancer (Sossey-Alaoui *et al.*, 2018; Yu *et al.*, 2013), pancreatic adenocarcinomas (Yoshida *et al.*, 2017),

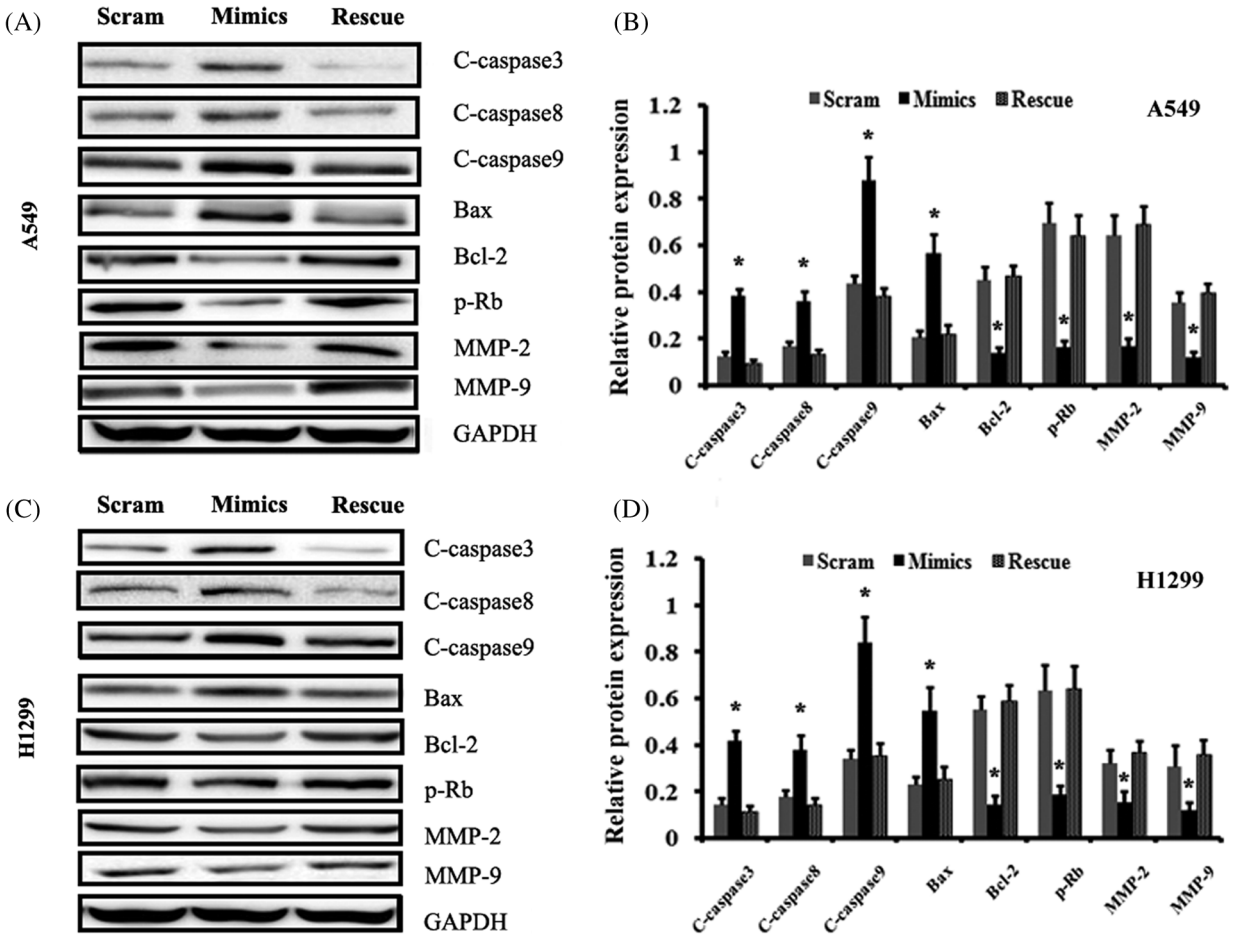

FIGURE 5. Effects of miR-16-5p on the apoptosis-, cell cycle- and invasion-related proteins via FERMT2.
(A) The apoptosis-, cell cycle- and invasion-related proteins were detected in A549 cells transfected with miR-16-5p scram, mimics and rescue (mimics + FERMT2-without-3'-UTR), respectively. (B) The quantified analyses of related proteins, detected by Western blot in A549 cells and indicated by the histogram. (C) The apoptosis-, cell cycle- and invasion-related proteins were detected in H1299 cells transfected with miR-16-5p scram, mimics and rescue (mimics + FERMT2-without-3'-UTR), respectively. (D) The quantified analyses of related proteins, detected by Western blot in H1299 cells and indicated by the histogram. C: cleaved, p-Rb: phosphate Rb, MMP: matrix metalloprotein. $^*p < 0.05$.

colorectal cancer cells (Lin *et al.*, 2017; Ma *et al.*, 2013; Ren *et al.*, 2015), prostate cancer (Sossey-Alaoui and Plow, 2016), hepatocellular carcinoma (Fan *et al.*, 2015; Lin *et al.*, 2017) and esophageal cancer (Wang *et al.*, 2017a; Zhang *et al.*, 2015). Considering the important roles of FERMT2 in cancer biology, it is not unexpected that a series of studies demonstrated that a few miRNAs could participate in the regulation of FERMT2 expression. For instance, a previous report showed that miR-200b resulted in the inhibition of EMT and metastasis by targeting FERMT2 (Sossey-Alaoui *et al.*, 2018; Zhang *et al.*, 2014). Similarly, miR-138 inhibited the metastasis of prostate cancer via the specific suppression of FERMT2 (Selth *et al.*, 2012; Sossey-Alaoui and Plow, 2016). In this study, the bioinformatics analysis indicated that FERMT2 might also be a possible target of miR-16-5p. This hypothesis was further validated by the luciferase reporter assay and related cotransfection tests. Our study gives new insight that the regulation of FERMT2, an activator of integrin in the development of cancers, might be a promising target because previous reports demonstrated that FERMT2 might exert a significant impact on poor prognosis by mainly modulating the integrin signaling pathway.

Some limitations in the present study should be mentioned for future investigations. First, the number of NSCLC patients enrolled in this study is limited. Thus, more extensive clinical trials should be warranted to make a more robust and convincing conclusion about the relation between miR-16-5p and NSCLC development and prognosis. Secondly, in this study, we only performed the assay of tumor formation in animal models. Considering the high metastasis potential of lung cancer, more proper methods, such as the tail vein injection, could be performed in further studies to explore whether miR-16-5p could influence lung cancer metastasis *in vivo*. Thirdly, the exact mechanisms and signaling pathways of the anti-tumor effect of miR-16-5p have not been fully explored. A more detailed understanding of the influences of cellular signal pathways induced by miR-16-5p will be beneficial to its better applications in NSCLC therapy.

In summary, our study revealed that miR-16-5p showed noticeable anti-cancer effects for NSCLC in cell lines, animal models, and available clinical samples, which may involve in the abilities to the apoptosis induction, the proliferation suppression, and the inhibition of invasion. Moreover,

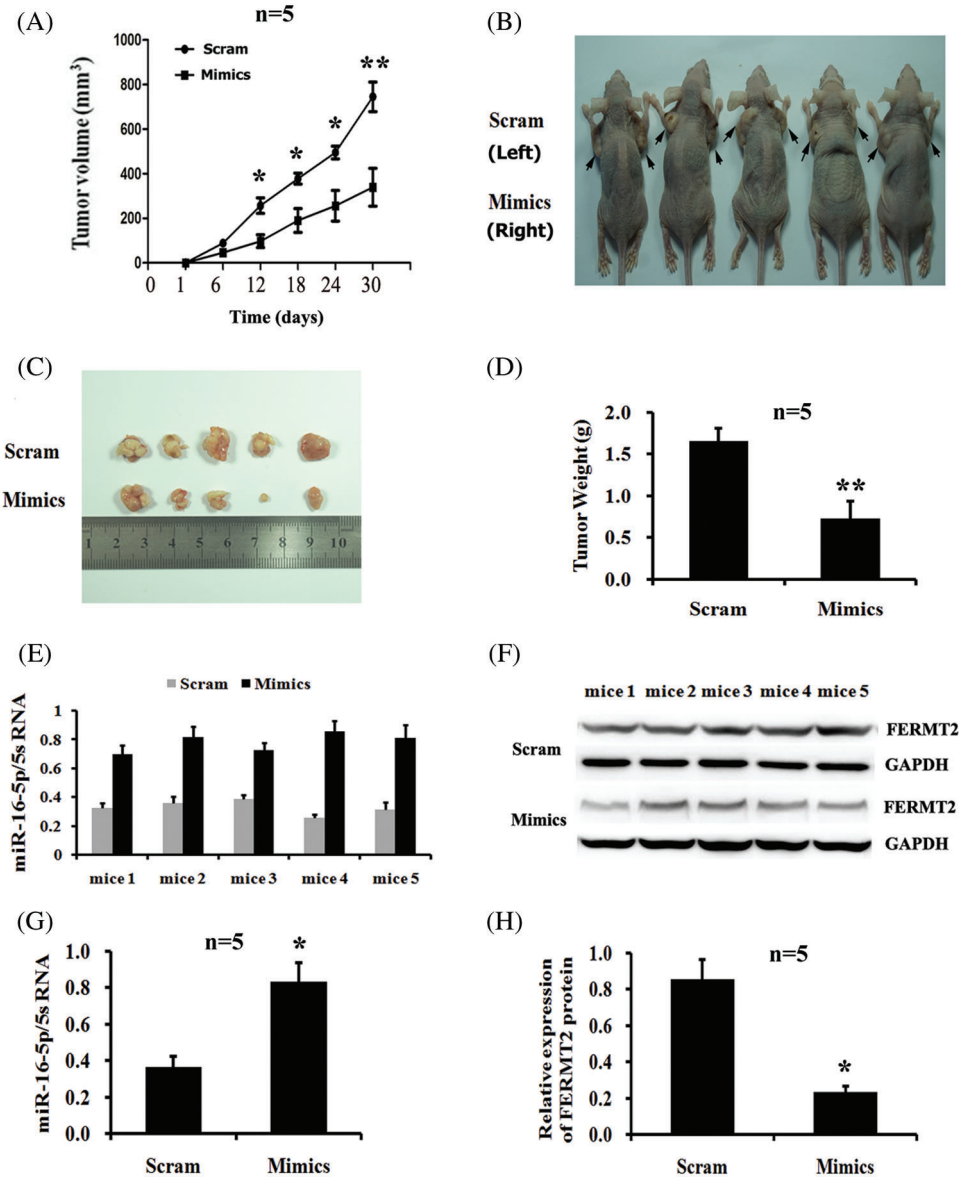

FIGURE 6. miR-16-5p inhibits lung cancer growth *in vivo*.
(A) Comparison of tumor volume in tumor-bearing mice between the miR-16-5p mimics group and the scram group. The tumor volumes in different groups were measured on days 1, 6, 12, 18, 24, and 30, respectively. (B) The representative photos of tumor-bearing mice on day 30. The black arrows indicated the growing tumor after the inoculation on day 30. (C) The removed tumors on day 30 from mice with different treatments were shown. (D) The histograms represent the quantitative data of tumor weights between groups. (E) The miR-16-5p expression levels in each removed tumors. (F) The levels of FERMT2 protein in each removed tumor detected by Western blot. (G) The analysis of miR-16-5p expression between scram and mimics group. (H) The analysis of FERMT2 protein levels between scram and mimics group.*$p < 0.05$, **$p < 0.01$.

definite evidence about the regulatory role of miR-16-5p targeting FERMT2 was also demonstrated. Our results provide further insight and new candidate targets for the promising therapeutic application in the treatment of NSCLC.

Availability of Data and Material: The datasets used and/or analysed during the current study are available from the corresponding author on reasonable request.

Author Contributions: FJ and JXH designed the study; JQG, YY, WZ, XY, YFY, and RMH performed the experiments; FJ, JXH, JQG, and ZHY wrote the manuscript; JXH, JQG, WZ, ZHY, and XY performed data analysis. All authors read and approved the final draft.

Funding Statement: This study was supported by grants from the National Natural Science Foundation of China (No. 81772281), the Shandong Province Taishan Scholar Project (No. ts201712067), the Major Research and Development Program of Shandong Province (No. 2017GSF18124) and the Natural Science Foundation of Shandong Province (No. ZR2020MH218).

Conflicts of Interest: The authors declare that they have no conflicts of interest to report regarding the present study.

References

Bentwich I, Avniel A, Karov Y, Aharonov R, Gilad S, Barad O, Barzilai A, Einat P, Einav U, Meiri E, Sharon E, Spector Y, Bentwich Z (2005). Identification of hundreds of conserved and nonconserved human microRNAs. *Nature Genetics* **37**: 766–770. DOI 10.1038/ng1590.

Bhattacharya R, Nicoloso M, Arvizo R, Wang E, Cortez A, Rossi S, Calin GA, Mukherjee P (2009). MiR-15a and MiR-16 control Bmi-1 expression in ovarian cancer. *Cancer Research* **69**: 9090–9095. DOI 10.1158/0008-5472.CAN-09-2552.

Bonci D, Coppola V, Musumeci M, Addario A, Giuffrida R, Memeo L, D'Urso L, Pagliuca A, Biffoni M, Labbaye C, Bartucci M, Muto G, Peschle C, De Maria R (2008). The miR-15a–miR-16-1 cluster controls prostate cancer by targeting multiple oncogenic activities. *Nature Medicine* **14**: 1271–1277. DOI 10.1038/nm.1880.

Cai B, Ma M, Chen B, Li Z, Abdalla BA, Nie Q, Zhang X (2018). MiR-16-5p targets SESN1 to regulate the p53 signaling pathway,

affecting myoblast proliferation and apoptosis, and is involved in myoblast differentiation. *Cell Death & Disease* **9**: 367. DOI 10.1038/s41419-018-0403-6.

Cimmino A, Calin GA, Fabbri M, Iorio MV, Ferracin M, Shimizu M, Wojcik SE, Aqeilan RI, Zupo S, Dono M, Rassenti L, Alder H, Volinia S, Liu CG, Kipps TJ, Negrini M, Croce CM (2005). miR-15 and miR-16 induce apoptosis by targeting BCL2. *Proceedings of the Nationl Academy of Sciences of the United States of America* **102**: 13944–13949.

Corthals SL, Jongen-Lavrencic M, de Knegt Y, Peeters JK, Beverloo HB, Lokhorst HM, Sonneveld P (2010). Micro-RNA-15a and micro-RNA-16 expression and chromosome 13 deletions in multiple myeloma. *Leukemia Research* **34**: 677–681. DOI 10.1016/j.leukres.2009.10.026.

Crino L, Weder W, van Meerbeeck J, Felip E, Group EGW. 2010. (2010). Early stage and locally advanced (non-metastatic) non-small-cell lung cancer: ESMO Clinical Practice Guidelines for diagnosistreatment and follow-up. *Annals of Oncology: Official Journal of the European Society for Medical Oncology* **21**: 103–115.

Croce CM (2009). Causes and consequences of microRNA dysregulation in cancer. *Nature Reviews Genetics* **10**: 704–714. DOI 10.1038/nrg2634.

Cui J, Li Q, Luo M, Zhong Z, Zhou S, Jiang L, Shen N, Geng Z, Cheng H, Meng L, Yi S, Sun H, Wu F, Zhu Z, Zou P, You Y, Guo AY, Zhu X (2018). Leukemia cell-derived microvesicles induce T cell exhaustion via miRNA delivery. *OncoImmunology* **7**: e1448330. DOI 10.1080/2162402X.2018.1448330.

Fan J, Im HJ, Liu Y, Chen J, Chen D, Xiao G, Ge YS, Liu D, Jia WD, Li JS, Ma JL, Yu JH, Xu GL (2015). Kindlin-2: A novel prognostic biomarker for patients with hepatocellular carcinoma. *Pathology, Research and Practice* **211**: 198–202. DOI 10.1016/j.prp.2014.09.011.

Guo CJ, Pan Q, Li DG, Sun H, Liu BW (2009). miR-15b and miR-16 are implicated in activation of the rat hepatic stellate cell: An essential role for apoptosis. *Journal of Hepatology* **50**: 766–778. DOI 10.1016/j.jhep.2008.11.025.

Ha TY (2011). The role of microRNAs in regulatory T cells and in the immune response. *Immune Network* **11**: 11–41. DOI 10.4110/in.2011.11.1.11.

Hanniford D, Zhong J, Koetz L, Gaziel-Sovran A, Lackaye DJ, Shang S, Pavlick A, Shapiro R, Berman R, Darvishian F, Shao Y, Osman I, Hernando E (2015). A miRNA-based signature detected in primary melanoma tissue predicts development of brain metastasis. *Clinical Cancer Research* **21**: 4903–4912. DOI 10.1158/1078-0432.CCR-14-2566.

Hao Z, Fan W, Hao J, Wu X, Zeng GQ, Zhang LJ, Nie SF, Wang XD (2016). Efficient delivery of micro RNA to bone-metastatic prostate tumors by using aptamer-conjugated atelocollagen *in vitro* and *in vivo*. *Drug Delivery* **23**: 874–881. DOI 10.3109/10717544.2014.920059.

Kloeker S, Major MB, Calderwood DA, Ginsberg MH, Jones DA, Beckerle MC (2004). The Kindler syndrome protein is regulated by transforming growth factor-β and involved in integrin-mediated adhesion. *Journal of Biological Chemistry* **279**: 6824–6833. DOI 10.1074/jbc.M307978200.

Kozomara A, Griffiths-Jones S (2011). miRBase: integrating microRNA annotation and deep-sequencing data. *Nucleic Acids Research* **39**: D152–D157. DOI 10.1093/nar/gkq1027.

Lewis DR, Chen HS, Cockburn MG, Wu XC, Stroup AM, Midthune DN, Zou Z, Krapcho MF, Miller DG, Feuer EJ (2018). Early estimates of cancer incidence for 2015: Expanding to include estimates for white and black races. *Cancer* **124**: 2192–2204. DOI 10.1002/cncr.31315.

Li H, Liu J, Chen J, Wang H, Yang L, Chen F, Fan S, Wang J, Shao B, Yin D, Zeng M, Li M, Li J, Su F, Liu Q, Yao H, Su S, Song E (2018). A serum microRNA signature predicts trastuzumab benefit in HER2-positive metastatic breast cancer patients. *Nature Communications* **9**: 1614. DOI 10.1038/s41467-018-03537-w.

Lin J, Lin W, Ye Y, Wang L, Chen X, Zang S, Huang A (2017). Kindlin-2 promotes hepatocellular carcinoma invasion and metastasis by increasing Wnt/β-catenin signaling. *Journal of Experimental & Clinical Cancer Research* **36**: 134. DOI 10.1186/s13046-017-0603-4.

Lu X, Zhou C, Li RF, Ye JW, Zhai WL (2018). Kindlin-2 promotes gallbladder cancer metastasis and invasion by inducing epithelial-mesenchymal transition. *ZhonghuaWaiKeZaZhi [Chinese Journal of Surgery]* **56**: 617–622.

Ma Q, Wang X, Li Z, Li B, Ma F, Peng L, Zhang Y, Xu A, Jiang B (2013). microRNA-16 represses colorectal cancer cell growth *in vitro* by regulating the p53/survivin signaling pathway. *Oncology Reports* **29**: 1652–1658. DOI 10.3892/or.2013.2262.

Paladini L, Fabris L, Bottai G, Raschioni C, Calin GA, Santarpia L (2016). Targeting microRNAs as key modulators of tumor immune response. *Journal of Experimental & Clinical Cancer Research* **35**: 103.

Pekarsky Y, Croce CM (2015). Role of miR-15/16 in CLL. *Cell Death & Differentiation* **22**: 6–11. DOI 10.1038/cdd.2014.87.

Pero-Gascon R, Sanz-Nebot V, Berezovski MV, Benavente F (2018). Analysis of circulating microRNAs and their post-transcriptional modifications in cancer serum by on-line solid-phase extraction-capillary electrophoresis-mass spectrometry. *Analytical Chemistry* **90**: 6618–6625. DOI 10.1021/acs.analchem.8b00405.

Qu Y, Liu H, Lv X, Liu Y, Wang X, Zhang M, Zhang X, Li Y, Lou Q, Li S, Li H (2017). MicroRNA-16-5p overexpression suppresses proliferation and invasion as well as triggers apoptosis by targeting VEGFA expression in breast carcinoma. *Oncotarget* **8**: 72400–72410. DOI 10.18632/oncotarget.20398.

Ren Y, Jin H, Xue Z, Xu Q, Wang S, Zhao G, Huang J, Huang H (2015). Kindlin-2 inhibited the growth and migration of colorectal cancer cells. *Tumor Biology* **36**: 4107–4114. DOI 10.1007/s13277-015-3044-8.

Renjie W, Haiqian L (2015). MiR-132, miR-15a and miR-16 synergistically inhibit pituitary tumor cell proliferation invasion and migration by targeting Sox5. *Cancer Letters* **356**: 568–578. DOI 10.1016/j.canlet.2014.10.003.

Rinnerthaler G, Hack LH, Gampenrieder S, Hamacher F, Hufnagl C, Hauser-Kronberger C, Zehentmayr F, Fastner G, Sedlmayer F, Mlineritsch B, Greil R (2016). miR-16-5p is a stably-expressed housekeeping microRNA in breast cancer tissues from primary tumors and from metastatic sites. *International Journal of Molecular Sciences* **17**: 156. DOI 10.3390/ijms17020156.

Rognoni E, Ruppert R, Fassler R (2016). The kindlin family: functions, signaling properties and implications for human disease. *Journal of Cell Science* **129**: 17–27. DOI 10.1242/jcs.161190.

Selth LA, Tilley WD, Butler LM (2012). Circulating microRNAs: Macro-utility as markers of prostate cancer. *Endocrine-Related Cancer* **19**: R99–R113. DOI 10.1530/ERC-12-0010.

Shi L, Jackstadt R, Siemens H, Li H, Kirchner T, Hermeking H (2014). p53-induced miR-15a/16-1 and AP4 form a double-

negative feedback loop to regulate epithelial-mesenchymal transition and metastasis in colorectal cancer. *Cancer Research* **74**: 532–542. DOI 10.1158/0008-5472.CAN-13-2203.

Sossey-Alaoui K, Plow EF (2016). miR-138-mediated regulation of KINDLIN-2 expression modulates sensitivity to chemotherapeutics. *Molecular Cancer Research* **14**: 228–238. DOI 10.1158/1541-7786.MCR-15-0299.

Sossey-Alaoui K, Pluskota E, Szpak D, Schiemann WP, Plow EF (2018). The Kindlin-2 regulation of epithelial-to-mesenchymal transition in breast cancer metastasis is mediated through miR-200b. *Scientific Reports* **8**: 7360. DOI 10.1038/s41598-018-25373-0.

Wang P, Zhan J, Song J, Wang Y, Fang W, Liu Z, Zhang H (2017a). Differential expression of Kindlin-1 and Kindlin-2 correlates with esophageal cancer progression and epidemiology. *Science China Life Sciences* **60**: 1214–1222. DOI 10.1007/s11427-016-9044-5.

Wang T, Hou J, Li Z, Zheng Z, Wei J, Song D, Hu T, Wu Q, Yang JY, Cai JC (2017b). miR-15a-3p and miR-16-1-3p negatively regulate Twist1 to repress gastric cancer cell invasion and metastasis. *International Journal of Biological Sciences* **13**: 122–134. DOI 10.7150/ijbs.14770.

Xia L, Zhang D, Du R, Pan Y, Zhao L, Sun S, Hong L, Liu J, Fan D (2008). miR-15b and miR-16 modulate multidrug resistance by targeting BCL2 in human gastric cancer cells. *International Journal of Cancer* **123**: 372–379. DOI 10.1002/ijc.23501.

Xu F, Zhang X, Lei Y, Liu X, Liu Z, Tong T, Wang W (2010). Loss of repression of HuR translation by miR-16 may be responsible for the elevation of HuR in human breast carcinoma. *Journal of Cellular Biochemistry* **111**: 727–734. DOI 10.1002/jcb.22762.

Yan Z, Liu Y, Wei Y, Zhao N, Zhang Q, Wu C, Chang Z, Xu Y (2017). The functional consequences and prognostic value of dosage sensitivity in ovarian cancer. *Molecular BioSystems* **13**: 380–391. DOI 10.1039/C6MB00625F.

Ye EA, Liu L, Jiang Y, Jan J, Gaddipati S, Suvas S, Steinle JJ (2016). miR-15a/16 reduces retinal leukostasis through decreased pro-inflammatory signaling. *Journal of Neuroinflammation* **13**: 305.

Yoshida N, Masamune A, Hamada S, Kikuta K, Takikawa T, Motoi F, Unno M, Shimosegawa T (2017). Kindlin-2 in pancreatic stellate cells promotes the progression of pancreatic cancer. *Cancer Letters* **390**: 103–114. DOI 10.1016/j.canlet.2017.01.008.

Yu Y, Wu J, Guan L, Qi L, Tang Y, Ma B, Zhan J, Wang Y, Fang W, Zhang H (2013). Kindlin-2 promotes breast cancer invasion via epigenetic silencing of the microRNA200 gene family. *International Journal of Cancer* **133**: 1368–1379.

Zhang H, Yang K, Ren T, Huang Y, Tang X, Guo W (2018). miR-16-5p inhibits chordoma cell proliferation invasion and metastasis by targeting Smad3. *Cell Death Disease* **9**: 680.

Zhang HF, Alshareef A, Wu C, Li S, Jiao JW, Cao HH, Lai R, Xu LY, Li EM (2015). Loss of miR-200b promotes invasion via activating the Kindlin-2/integrin beta1/AKT pathway in esophageal squamous cell carcinoma: An E-cadherin-independent mechanism. *Oncotarget* **6**: 28949–28960.

Zhang HF, Zhang K, Liao LD, Li LY, Du ZP, Wu BL, Wu JY, Xu XE, Zeng FM, Chen B, Cao HH, Zhu MX, Dai LH, Long L, Wu ZY, Lai R, Xu LY, Li EM (2014). miR-200b suppresses invasiveness and modulates the cytoskeletal and adhesive machinery in esophageal squamous cell carcinoma cells via targeting Kindlin-2. *Carcinogenesis* **35**: 292–301.